



## REGIONAL SELF-POTENTIAL ANOMALIES AT KILAUEA VOLCANO

By Dallas B. Jackson and James Kauahikaua

### ABSTRACT

Self-potentials (SP) at Kilauea Volcano, when referenced to the potential at sea level, appear as a broad, negative bowl-shaped anomaly with smaller wavelength anomalies that are positive-trending, but not necessarily of positive amplitude, superimposed over thermal volcanic features. To a first approximation, the broad-wavelength negative anomaly is inversely correlated with topography. Plots of SP versus topography and (or) vadose-zone thickness determined from vertical electrical soundings show linear, sometimes segmented, correlations along four lengthy SP profiles on Kilauea. The slopes of the correlation lines are used to calculate an apparent water-table elevation along the entire profile. When compared with surface geology and nearby well data, the apparent water table is reasonable. The ground water table is near sea level for most areas south of the middle and lower east rift zone and at the boundary between the southwest rift zone of Kilauea and the southeast flank of Mauna Loa near the coast. By contrast the profiles show that water may be impounded to high elevations within the east rift zone, both east and west of the upper east rift zone, and beneath the summit region. The water table is also elevated beneath the southwest flank of Kilauea.

### INTRODUCTION

The self-potential or spontaneous-potential (SP) method measures naturally occurring electric-field potentials that exist at the Earth's surface. Extensive potential-field mapping on Kilauea shows there is a direct relation between volcanic structure and SP field distribution at the summit of Kilauea Volcano (Zablocki, 1976). An SP map of the intersection of the lower east rift zone of Kilauea with the coast (Zablocki, 1977) and two new profiles, each referenced to the potential at sea level, show that the regional (that is, the long-wavelength) portion of SP appears strongly correlated with topography. Zablocki suggested that a more meaningful correlation is between SP and vadose-zone thickness. In this paper we will first discuss SP-measurement techniques and possible measurement errors in order to demonstrate that our field measurements genuinely reflect natural Earth potentials. Then we will quantify the relation of SP magnitude to topography and (or) thickness of the vadose zone in an attempt to isolate a cause of regional SP.

### MEASUREMENT TECHNIQUES

The measurement of self-potential is quite simple, requiring only a high-impedance millivoltmeter, nonpolarizing electrodes, and

approximately 2 km of insulated single-conductor wire. It is desirable to space reference points as far apart as practical to keep cumulative errors to a minimum, but to make measurements also at smaller intervals between reference points. For example, we commonly make measurements at 100-m intervals, but only move reference points every 1.5 km.

A typical nonpolarizing electrode consists of a bare copper strip immersed in a supersaturated copper-sulfate solution in a porous ceramic cup. The cup has sides wrapped in fiberglass for added strength and can be fabricated with a large bottom surface area to improve electrical contact with the ground.

At Kilauea, it is essential that a very high impedance millivoltmeter be used. The electrical resistance between the electrodes and the earth can easily vary between a few tens of ohms for deeply weathered or altered ash and lava flows to megaohms for dry sand and ash or unweathered lava flows. A millivoltmeter input impedance several orders of magnitude larger than the largest expected electrode resistance insures that errors due to electrode resistance are kept small. We use a very simple system designed by Zablocki (1976) that incorporates an electrometer amplifier ( $10^{14}$  ohms impedance) with a filtered input to reject AC signals and a digital display of 1 to 999 mV. The amplifier has an input bias current of only  $10^{-14}$  A, an important consideration because large bias currents will polarize the measuring electrodes.

In the field, a reference electrode is established and a second electrode is moved successively to each measurement site. The electrode is positioned by simply placing it on the ground and rotating it to make contact with the soil-moisture layer that is usually present just a few millimeters beneath the surface. Only in rare cases is it necessary to disturb the ground surface by digging to make adequate contact. If a reading is not repeatable to within 1–2 mV or is unstable, we assume that contact resistance is probably very high, and readings are discontinued at that location. In areas where soil texture varies from very coarse ash (commonly well drained and dry) to finer grained ash, the electrical contact may improve at the next reading position and readings are continued. The most common cause of high contact resistance is usually a long period of drought, in which rainfall has been too low to maintain fluid continuity between the ground surface and the film of water that is always present in the vadose zone (unsaturated zone between the ground surface and the water table).

Water is almost never added to the ground surface to improve electrical contact because watering of electrodes can produce extraneous potentials and a complex voltage drift (one exception to this is

described later). A good example of such behavior is shown in Corwin and Hoover (1979). The same considerations do not apply to the surfaces of fresh lava flows. There a moist rag or a sponge pushed into cracks in the flow surface is usually sufficient to lower contact resistance enough to give readings repeatable to within 1–2 mV.

The only exception we have made to the rule of not watering electrodes is on a monitored profile on Mauna Loa Volcano at the 3,400-meter elevation (Lockwood and others, 1985), where rainfall is very low most of the year. Even with a high impedance millivoltmeter, stable readings are normally not possible in this environment. As an experiment, water was added at each position that a reading was to be made, and then the SP drift was observed. After about 2 hours, the initial rapid potential drift (that began at about 10 mV/min) stopped; readings thereafter appeared stable and the profile was measured. A repeat of the profile 24 hours later gave readings that differed by less than 10 mV from the first measurements. Although very time-consuming, watering of electrodes appears to be permissible under these circumstances and may be the only way data can be collected in extremely dry areas.

### POSSIBLE MEASUREMENT ERRORS

Measurement errors related to mapping can be caused by (1) poor electrical contact with the ground surface in extremely dry areas, as discussed above; (2) failure to reoccupy electrode positions exactly when changing references on a traverse; (3) use of electrodes that are polarized; and (4) telluric currents.

#### INEXACT REFERENCE ELECTRODE POSITIONING

The failure to reoccupy exact reference-electrode positions can produce measurement errors in areas of anomalous gradients (for example, on the flanks of short-wavelength high-amplitude anomalies). This is a simple error to correct because high gradient areas are easily recognized during data collection and can be avoided as reference locations. Typical closures calculated for a wide variety of grounding conditions have always been less than 10 mV/km. Such errors are insignificant in mapping large potential changes; we are convinced that serious reference-electrode positioning errors can generally be avoided with a bit of care.

#### ELECTRODE BIAS

Copper sulfate nonpolarizing electrodes can sometimes drift from a balanced state (zero difference between electrodes) as they age or if they are contaminated. Such offsets can range from common values of 1–10 mV to more than 50 mV in extreme cases. To correct this, readings may be numerically compensated for the polarization by linearly distributing potential differences along a traverse, or matched pairs of electrodes with minimal bias can be selected from a large set of electrodes maintained for mapping.

### TELLURIC CURRENTS

Temporal variations of the Earth's magnetic field induce current flow in the Earth (telluric currents). The fluctuations of the electric field range in duration from milliseconds to centuries and can produce electric-field gradients of several hundred millivolts per kilometer over highly resistive terrain (Keller and Frischknecht, 1966), as is common in the continental interior. However, in an island setting such as Hawaii, where the rocks may also be highly resistive, the telluric currents tend to flow around the island in the conductive ocean water (Klein and Larson, 1978). At Kilauea, tellurics are generally too small (less than 1 mV/km) to be seen while SP readings are being made. Longer term and higher amplitude variations could conceivably introduce errors in SP traverse readings if their rate of change is such that measurable electric-field changes are produced during the time required for successive profile readings (about 4–8 minutes). The magnitude of potentials related to telluric currents is approximately proportional to the length of line on which they are recorded; therefore, the greater the distance between the reference and measuring electrodes the larger will be the error.

There is no way to quantitatively correct for changes related to telluric currents. However, one can attempt to estimate the perturbations and then dismiss them as sources of error if they are small. We estimate that a 1.5-km profile segment should take no longer than 2 hours to sample at 100-m intervals. The best set of published telluric measurements at Kilauea are those by Zablocki (1980) for potentials continuously recorded over 5 months in 1974 on two stationary orthogonal lines near the upper-east-rift-zone (UERZ) profile in figure 40.1. During that study, the largest excursions recorded over a 2-hour period were 25 mV/km. The great majority of such excursions were of about 10 mV/km or less. Therefore, for the worst case, it might be possible to have an error of about 40 mV over the 1.5 km segment. When mapping anomalies with amplitudes of several hundred millivolts, even this worst case would not seriously affect the results.

### GEOLOGIC SP SOURCES

Two source mechanisms seem to be capable of generating large self-potentials. The first mechanism, electrokinetic coupling or streaming potentials, is related to the circulation of fluids through porous rock (Sill, 1983). The second mechanism, thermoelectric coupling, can generate anomalous potentials at the ground surface from thermal gradients near dike-like heat sources (Fitterman, 1983).

#### THERMOELECTRIC COUPLING

Rocks are capable of producing an electric potential gradient in response to a thermal gradient. Fitterman (1984) has shown that the necessary conditions for the generation of a thermoelectric SP anomaly are a heat source and a change in the thermoelectric coupling property (ratio of voltage change to temperature change) in the vicinity of the heat source within the earth. Examples of theoretical SP anomalies produced by various heat sources and

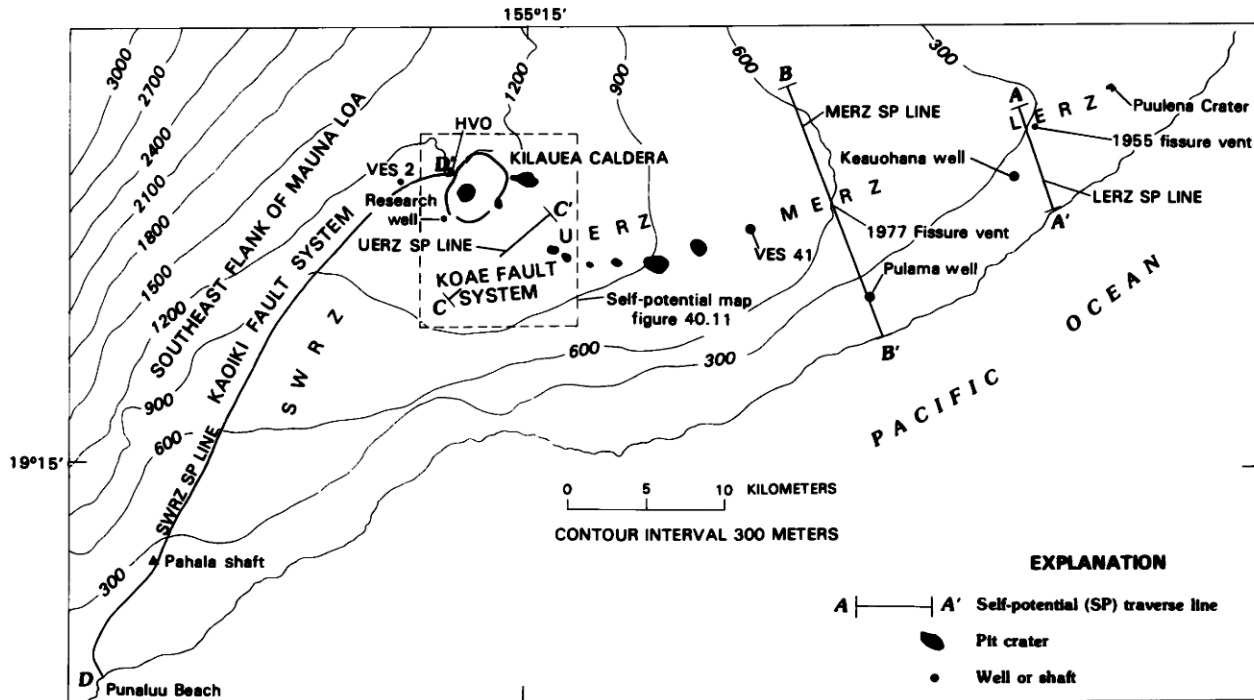


FIGURE 40.1.—Self-potential (SP) lines and major geologic features on Kilauea Volcano. SWRZ, southwest rift zone; UERZ, upper east rift zone; MERZ, middle east rift zone; LERZ, lower east rift zone.

various distributions of thermoelectric coupling property are shown in Fitterman (1978, 1979, 1983, 1984). Typical Earth heat sources in a volcanic terrain are buried magma bodies.

#### ELECTROKINETIC COUPLING

Rocks can also be a source of electric potential gradients if subjected to fluid flow within the rock pores. Necessary conditions for production of an electrokinetic SP anomaly are a fluid pressure gradient and a change in the electrokinetic coupling property (ratio of voltage change to pressure change) in the vicinity of the pressure gradient. Sill (1983) models various geometries for point pressure sources (abstract representations of pumping wells or springs) and for fluid which is convecting (Sill, 1982). As a rule, electric potentials become more positive in the direction of flow. In a uniform halfspace with nonzero electrokinetic coupling properties, positive anomalies are produced over a convection cell which is flowing vertically upward at the center and over a point source (such as a pumping well) in which fluid is flowing toward the point source. Electrokinetic causes have been hypothesized for SP anomalies observed in Yellowstone National Park (Zohdy and others, 1973) and Long Valley caldera, California (Anderson and Johnson, 1976).

#### SP CORRELATIONS WITH TOPOGRAPHY

A negative correlation between ground elevation (topography) and self-potential has been recognized for many years (Poldini, 1939; Yungul, 1950). Such correlations have been observed in many places, including Adagdak Volcano, Adak Island, Alaska (Corwin and Hoover, 1979), Hualalai Volcano, Hawaii (Jackson and Sako, 1982), and Kilauea Volcano (Zablocki, 1977).

The correlation with topography was initially thought to be due to the flow of nonthermal subsurface water (Poldini, 1939; Yungul, 1950) presumably through an electrokinetic mechanism. More recently, Zablocki (1978) proposed that the vertical descent of meteoric water through the vadose zone to the water table is the source mechanism, implying that SP intensities should actually be correlated to the underlying vadose-zone thickness, not to topography.

SP is clearly correlated with topography where the water table is horizontal near the coast. When both topography (meters) and SP (millivolts) are referenced to sea level and are plotted against one another, linear trends are commonly found which can be described by an equation of the form

$$SP = \text{ground elevation} \times C_c + A,$$

where  $C_e$  is the coefficient relating SP and ground elevation and  $A$  is the Y-axis intercept. For coastal areas where the water table is horizontal and at sea level, the constant ( $A$ ) is zero. However, more than one value of the coefficient is found even for single SP profiles, indicating that SP is not primarily related to ground elevation but possibly instead to vadose zone thickness.

SP should also be plotted against vadose-zone thickness where data are available, such as vertical electrical (Schlumberger) soundings or drilled wells. Linear trends of the form

$$SP = \text{vadose zone thickness} \times C_v + A$$

should be sought, where  $C_v$  is the constant of proportionality between SP and vadose-zone thickness. The constant,  $A$ , should be zero in this case. Unfortunately, measurements of vadose-zone thickness are not as common as ground elevation measurements. Only one of the four profiles (UERZ) presented in this paper has enough measurements of vadose-zone thickness available to determine a value for  $C_v$ . The other profiles have only one or two vadose-zone thickness determinations. For those, the SP correlation with topography was determined at the coast where the water table is almost certainly horizontal and at sea level. Using the value of  $C_e$  so derived, which in this case is equivalent to  $C_v$ , we calculated apparent water-table elevations for the entire profile by means of the equation

$$\text{water-table elevation} = \text{ground elevation} - SP/C_v.$$

These calculated values were then compared with the few known water-table elevations to test the supposition that regional scale SP is related more directly to vadose-zone thickness than to topography.

Many shorter wavelength SP anomalies may also be related to local vadose-zone thickness variations. For the most part, these anomalies are positive, monopolar, and located over thermal areas. Zablocki (1978, p. 747) proposes that these anomalies "may simply reflect the shallow depths to which cool meteoric water may descend before encountering higher temperature fluids rising above a deeper heat source. Enhancement of the anomalies may result from the ascending water vapor over the thermal area and from a large flux of liquid-phase water diverted laterally downward along the immediate flanks of the thermal zone." These short-wavelength anomalies may also be produced by thermoelectric sources (heat produced by intrusive magma) or electrokinetic sources other than the descent of meteoric water (such as thermal convection of water below the water table).

### SP PROFILES MEASURED ON KILAUEA VOLCANO

The following section describes four SP profiles measured on long traverses over large changes either in elevation and (or) in thickness of the vadose zone.

#### MIDDLE EAST RIFT ZONE (MERZ)

A 17-km traverse was run from the ocean up the south flank and across the MERZ to the north flank of the rift (fig. 40.2; see

also fig. 40.1). This SP profile has the form of a broad potential low, becoming increasingly more negative relative to sea level as the rift zone is approached. A positive-trending, high-amplitude (about 1,000 mV relative to adjacent levels) SP anomaly about 3–4 km wide is present over the active rift zone. Prominent but narrow positive-trending inflections on the SP profile also mark a fissure associated with a 1977 eruption (10.2 km from the SW. end of the profile at the coast), a 1963 eruptive fissure (10.7 km), and a 1968 fissure (11.5 km) that erupted lava from vents about 1.5 km on either side of the profile.

A zone with a good correlation ( $C_e = -1.7$  mV/m) between topography and SP (circles on fig. 40.3) extends approximately 8.2 km from the coast to the northwest beyond the large fault scarps of the steep south flank. We infer from well data (Pulama well) at about the 2.8-km position on the profile that the water table is nearly horizontal and at sea level in this portion of the profile (State of Hawaii Department of Land and Natural Resources, 1970). The linear gradient of  $-1.7$  mV/m ends at 8.2 km where the large positive-trending SP anomaly over the active rift begins (fig. 40.2).

At 10.2 km, the potentials rise above the zero reference by about 200 mV for a short distance across the 1977 fissure vent. Similar short-wavelength (<1 km) monopolar features (fig. 40.2) are also associated with the 1963 vent and the 1968 fissure. A fourth short-wavelength anomaly, similar in appearance to those at the 1963 vent and 1968 fissure, occurs on the SP profile between 13 km and 14 km. This feature is not directly associated with any surface feature but is only about 0.5 km beyond the northern limit of a horst-and-graben structure that is probably related to shallow intrusions of prehistoric (before the first recorded MERZ eruption in 1790) age but less than 300 years old (Holcomb, 1980).

Northwest of the rift zone (beyond any surface expression of eruptive features), the SP gradually increases (fig. 40.2). The slope of SP plotted against elevation for this section of the profile is about  $-4.4$  mV/m (fig. 40.3), steeper than that measured southeast of the rift zone. Calculations of apparent water-table elevations using the coefficient of  $-1.7$  mV/m are shown in figure 40.2.

#### LOWER EAST RIFT ZONE (LERZ)

The LERZ SP mapped by Zablocki (1977, fig. 2), has basically the same pattern of potential distribution as the MERZ. All areas not associated with obvious thermal features are more negative than potentials at sea level. Only two areas, one associated with a 1955 fissure vent (fig. 40.4) and the other associated with a prehistoric pit crater, Puulena (located on fig. 40.1; data not shown), are positive relative to sea level (about 50 mV). The one data set that Zablocki (1977, fig. 4) examined for a topographic-SP correlation runs from the ocean to a 1955 fissure vent and has a correlation coefficient ( $C_e$ ) of  $-1.8$  mV/m (fig. 40.5). This is comparable to the correlations we have found for other parts of the volcanic edifice where we believe the water table to be nearly horizontal. Using the SP and topographic data from Zablocki's figure 4, we have calculated and plotted the apparent water table along the profile (fig. 40.4).

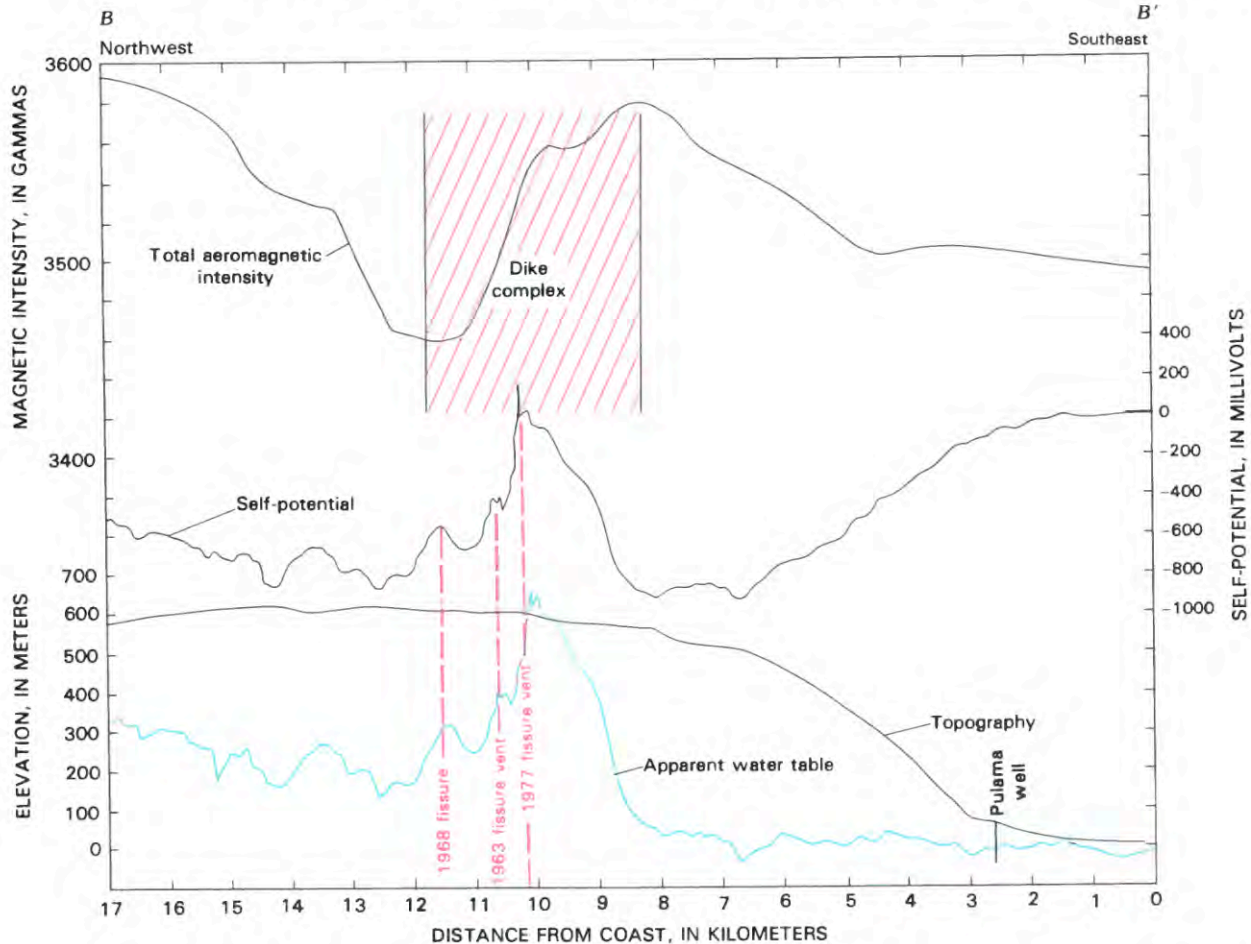


FIGURE 40.2.—Topography, self-potential, apparent water table, and total magnetic intensity (aeromagnetic) for profile B–B' across the middle east rift zone of Kilauea Volcano. See figure 40.1 for profile location.

#### UPPER EAST RIFT ZONE (UERZ)

The SP anomaly over the UERZ (fig. 40.6) has much the same form in cross section as the SP profile across the MERZ in figure 40.2, that is, a major positive anomaly (relative to nearby potentials) flanked by adjacent major potential lows. The UERZ anomalies are correlated with pit craters as far downrift as Pauahi and with fissure vents (not visible at the figure scale) northeast of Pauahi as far east as the right edge of the figure.

A plot of elevation against SP for the UERZ profile (fig. 40.7) shows no clear correlation. Lacking more direct measures of vadose-zone thickness for this profile, we choose to use interpretations from nearby vertical electrical soundings (VES). VES 1, 3, and 17 (fig. 40.8; locations shown in fig. 40.11) show the vadose zone to be 480, 230, and 690 m thick, respectively. These values are plotted with the corresponding SP values in figure 40.7 along with a line showing the determined value of  $C_v$ , the correlation

coefficient of vadose vent thickness to SP, of  $-3.6$  mV/m. An apparent water table calculated using this value is shown in figure 40.6.

#### SOUTHWEST RIFT ZONE (SWRZ)

An SP profile from ocean to the summit of Kilauea (fig. 40.1, left side) is shown in figure 40.9. This profile is 43 km long and extends from Punaluu Beach on the southwest flank of Kilauea to the Hawaiian Volcano Observatory (HVO) on the northern rim of the caldera at 1,246-m elevation. As in the MERZ profile, potentials become increasingly more negative as elevation increases. The SP at the end point of the profile (HVO) is  $-1,430$  mV relative to sea level.

The Punaluu-summit profile parallels the SWRZ of Kilauea and the Kaoiki fault zone and runs for its entire length over a

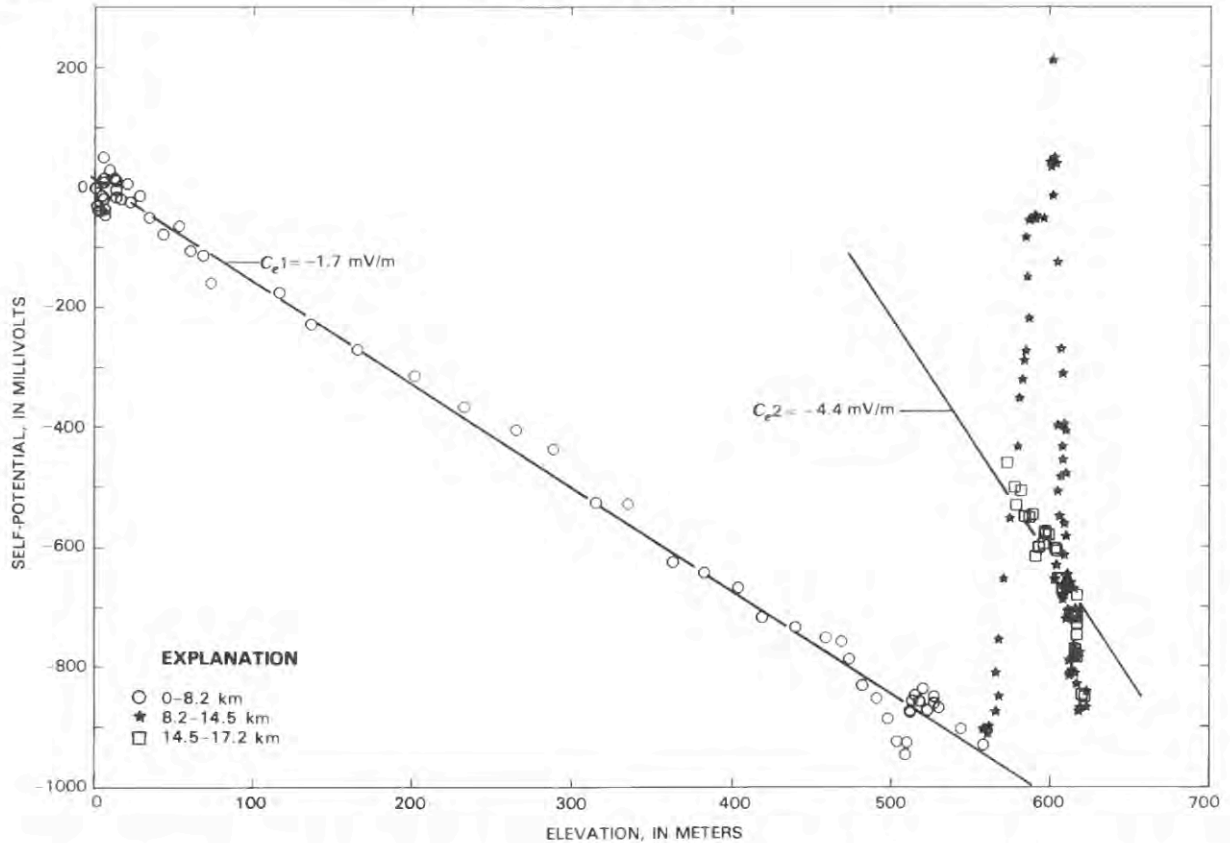


FIGURE 40.3.—Plot of elevation versus self-potential for the 17-km MERZ profile shown in figure 40.2. The lines show linear correlations (graphically determined) between self-potential and elevation with coefficients ( $C_e$ ) of  $-1.7$  mV/m and  $-4.4$  mV/m.

section in which flows from Kilauea and Mauna Loa interfinger. The Kaoiki fault zone extends from just north of Kilauea summit nearly to Pahala, and in places seems to act as a hydrologic barrier between Kilauea and the south flank of Mauna Loa (HVO unpublished electrical sounding data, 1980).

A plot of topography against self potential (fig. 40.10) shows three distinct values of  $C_e$  (labeled  $C_{e1}$ ,  $C_{e2}$ , and  $C_{e3}$ ) increasing in value from the coast toward the summit:

(1)  $C_{e1}$ , from the coast to 500-m elevation, about 6 km above the town of Pahala, has a value  $-0.6$  mV/m.

(2)  $C_{e2}$ , from 500-m elevation to 1,100-m elevation, about 2 km from the summit caldera, has a value of  $-1.6$  mV/m; this is approximately the same as observed on both the south flanks of the MERZ ( $-1.7$  mV/m) and the LERZ ( $-1.8$  mV/m).

(3)  $C_{e3}$ , from the 1,100-m elevation to the caldera rim at HVO, has a value of  $-3.2$  mV/m.

Apparent water-table values along this profile were calculated three times, once for each of the  $C_e$  values determined above. Only those calculated for  $C_{e2}$  and  $C_{e3}$  were hydrologically reasonable

(that is, they did not go below sea level); both these apparent water-table plots are shown in figure 40.9.

#### DISCUSSION

Three of the four self-potential profiles at Kilauea, one from the summit down the SWRZ, another from the MERZ down the south flank, and a third covering most of the LERZ (Zablocki, 1977), all referenced to sea level, clearly show that the edifice of Kilauea sits within a broad potential low. Within this low, and coinciding with the active elements of the volcano (rift zones, intrusions, pit craters, and fissure vents) are large self-potential highs that, with few exceptions, are nonetheless still negative with respect to sea level.

In each of these three areas, at places where it is reasonable to expect a nearly horizontal water table, ground elevation shows an excellent correlation to self-potential with a coefficient of approximately  $-1.7$  mV/m. Along the UERZ profile, a good correlation was found between vadose-zone thickness and SP with a coefficient of  $-3.6$  mV/m.

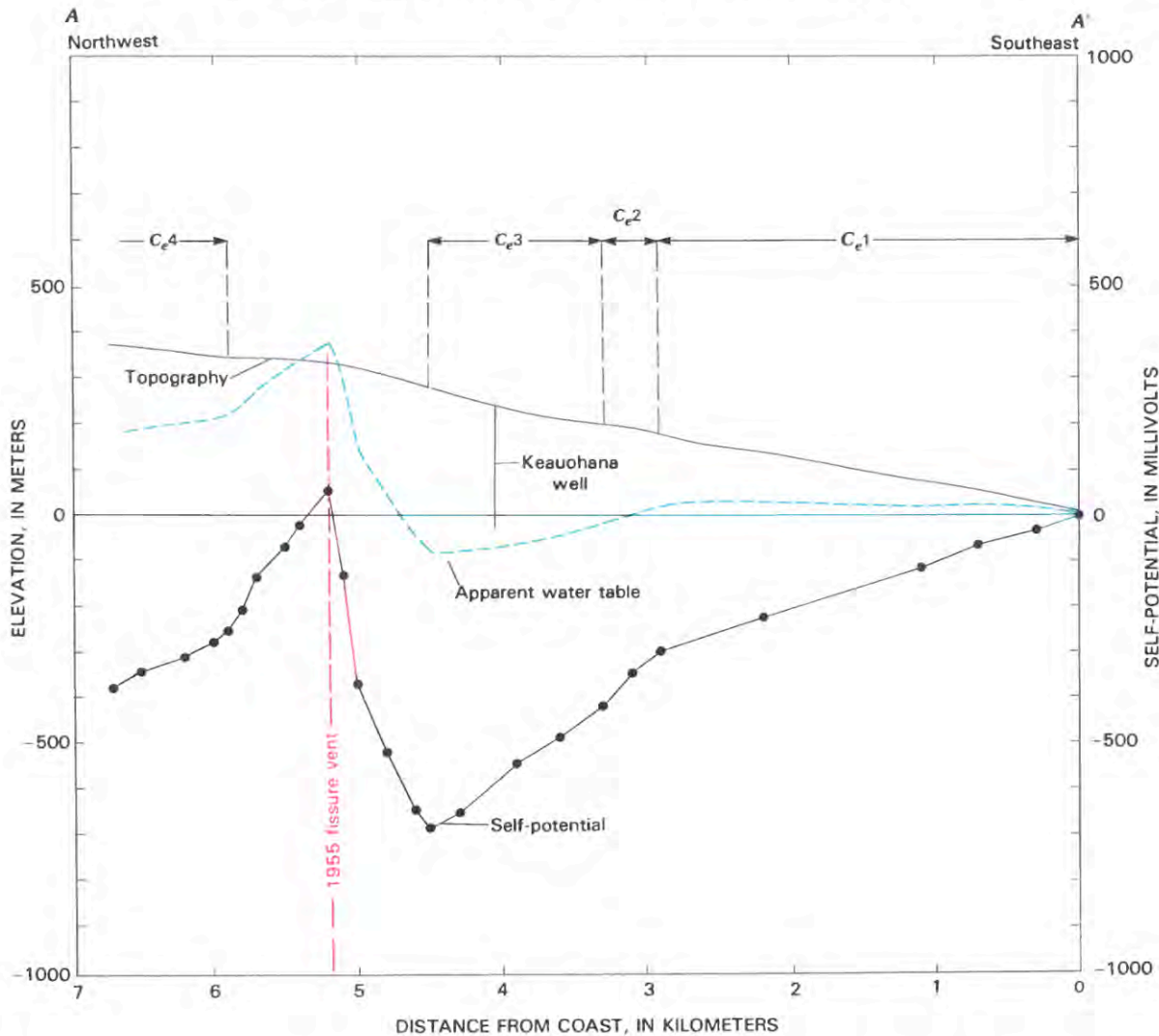


FIGURE 40.4.—Topography, apparent water table, and self-potential for profile A–A' on the lower east rift zone of Kilauea Volcano. Self-potential and topography digitized from Zablocki (1977, fig. 2). Segments of the profile that correspond to different linear correlations ( $C_e1$  through  $C_e4$  on fig. 40.5) are shown. See figure 40.1 for profile location.

We believe, along with Zablocki (1978), that the regional pattern of SP is more directly related to the distance to which water can percolate vertically through the vadose zone before reaching the water table than it is to topography. We recognize that our analysis is not definitive but only indicative. Inconsistencies can be shown in the correlation of SP to topography, and those inconsistencies indicate a relationship of SP to vadose-zone thickness. The exact mechanism by which the negative potentials are generated is not known, but it is probably related to streaming potentials generated within the vadose zone by water moving downward.

If we suppose a valid relationship between vadose-zone thickness and self-potential, then self-potentials referenced to sea level at

known elevations may be converted to apparent water-table depths. Circumstantial evidence that such a conversion is valid would come from any agreement of these apparent water-table elevations with actual determinations (well data and electrical resistivity soundings) at the same sites.

#### MIDDLE-EAST-RIFT-ZONE PROFILE

The apparent water-table elevations remain near sea level from the shore inland to the edge of the dike complex and then increase rapidly toward the 1977 eruptive fissure (fig. 40.2). Northwest of the 1977 fissure, apparent water-table elevations decrease to a point

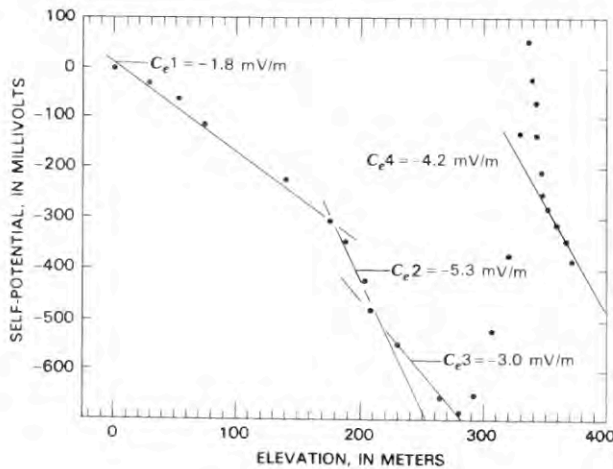


FIGURE 40.5.—Plot of elevation versus self-potential for the LERZ profile shown in figure 40.4. Four linear segments and the values of their correlation coefficients ( $C_e1-C_e4$ ) are shown. Correlation lines are graphically determined.

about 14 km from the coast, from where they rise slowly to the end of the profile.

The apparent water-table elevations rise dramatically along the MERZ profile over the portion of the rift underlain by a dike complex. The long-wavelength (about 3 km) high in SP over the dike complex and the shallow apparent water table derived from the SP within this high are best explained as a thinning of the vadose zone caused by impoundment of ground water by dikes within the rift zone. An elevated water table within the rift is confirmed by VES 41 approximately 5 km uprift from the MERZ profile. For VES 41, at 740-m elevation (figs. 40.1 and 40.8), the water table is interpreted to be at 390 m above sea level. Although VES 41 is evidence of elevated water within this structure, its location is too far uprift to allow direct comparison with the MERZ profile.

At 8.2 km from the shore on the profile is the southern boundary of the active rift as indicated by the southernmost occurrence of pyroclastic cones in this area (Holcomb, 1980, p. 167). A low-level total-intensity aeromagnetic profile of the east rift zone (fig. 40.2; see also Flanigan and Long, chapter 39) also shows that the southern margin of the dike complex is about 8.2 km from the coast,

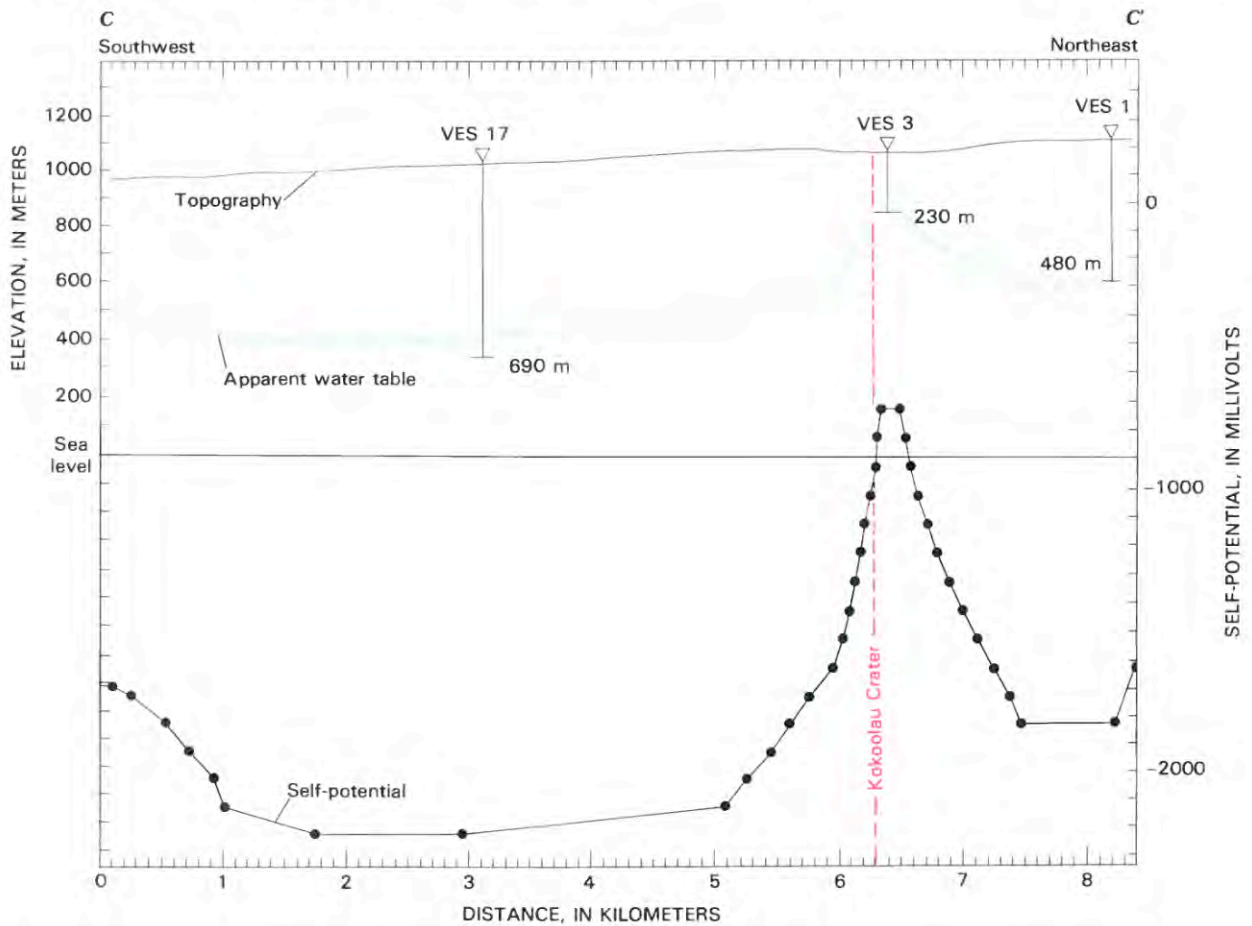


FIGURE 40.6.—Topography, apparent water table, and self-potential for profile C-C' on the upper east rift zone of Kilauea Volcano. See figures 40.1 and 40.11 for profile location and figure 40.8 for VES interpretations.

and the complex extends to at least the 11.5-km position on the profile. The interpreted dike-complex margins on the aeromagnetic profile correspond to the crest of the aeromagnetic high to the southeast and the trough of the aeromagnetic low to the northwest (fig. 40.2).

The point at which the apparent water table rises above the ground surface (fig. 40.2) coincides with a short-wavelength (<1.5 km) anomaly that is positive relative to sea level and thus cannot be attributed to vadose-zone thinning. Because the short-wavelength anomaly coincides with a fissure vent, it must be caused by a thermoelectric or electrokinetic mechanism (or a combination of both) associated with the subsurface heat source responsible for the fissure. The other short-wavelength anomalies along the profile that are associated with fissure vents may also not be related directly to the vadose zone.

The more gradual decrease of apparent water-table elevation northwest of the 1977 fissure may be the result of a leaky dike system that cannot support the same hydraulic head that is maintained southeast of the fissure. The gradual rise of the apparent water table at the northwest end of the profile may be evidence for high-level impoundment of ground water by an older ERZ dike system or possibly by older dikes related to an aeromagnetic lineation that branches off from the Mauna Loa northeast rift zone 15 km from the summit and parallels the north side of the Kilauea ERZ (Flanigan and Long, chapter 39).

#### LOWER-EAST-RIFT-ZONE PROFILE

The apparent water table calculated for the LERZ profile (fig. 40.4) begins at zero elevation at the coast then dips as much as 100 m below sea level (4.5 km inland) in the area immediately southeast of a 1955 fissure vent (at 5.2 km). The Keauohana well located to the south of the rift just off the profile at the 4-km position shows that the water table is about 1 m above sea level (State of Hawaii Department of Land and Natural Resources, 1970), though the apparent water table is about 100 m below sea level. The discrepancy implies that this portion of the profile either is affected by SP mechanisms associated with the 1955 vent more than by vadose-zone variations or that it has a different coefficient for the correlation of vadose-zone thickness and SP.

Northwest of the fissure vent and within the rift, the apparent water table is elevated nearly 200 m above sea level; this is consistent with interpretations of elevated water tables in the middle and upper east rift. Self-potentials associated with the 1955 fissure vent and (or) a changing coefficient,  $C_v$ , may also bias the apparent water-table depths northwest of the vents, but we do not know how much. A discrepancy is obvious at the position of the fissure vent, where the apparent water table is about 30 m above the ground surface. Here again we believe that these eruptive-vent anomalies, which are generally short wavelength, are due to thermoelectric or electrokinetic phenomena associated with subsurface heat sources.

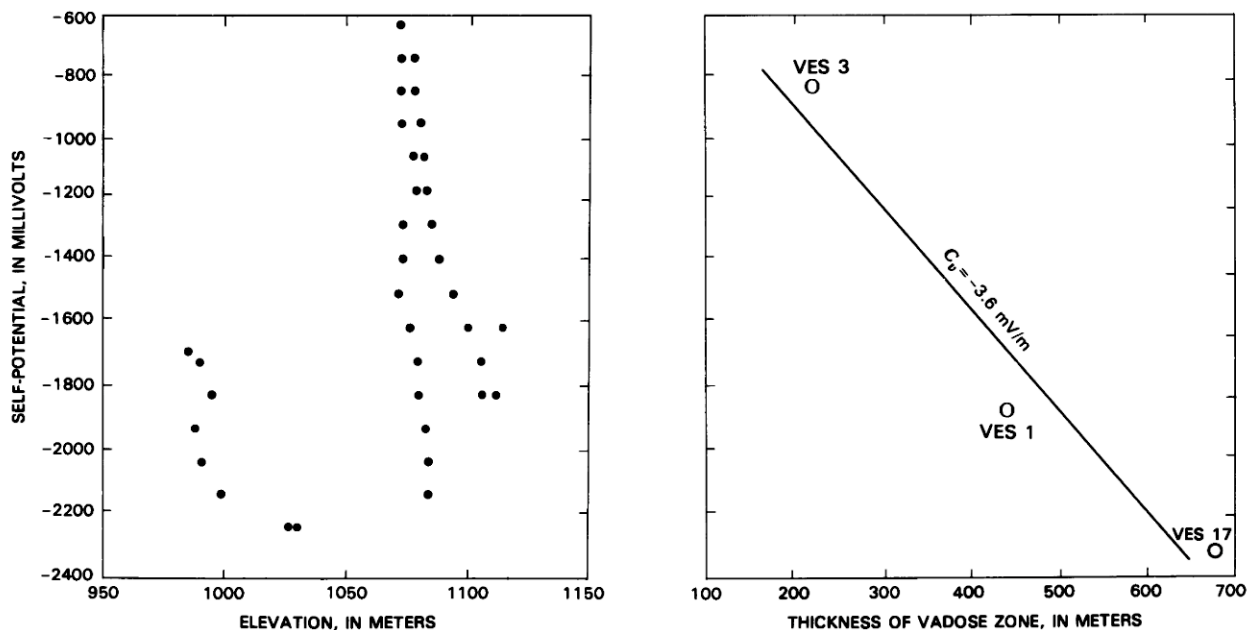


FIGURE 40.7.—Plots of self-potential versus elevation and versus vadose-zone thickness for the UERZ profile shown in figure 40.6. In the latter plot, the correlation of self-potential and vadose zone thickness is derived from VES interpretations discussed in the text. Correlation line is graphically determined.

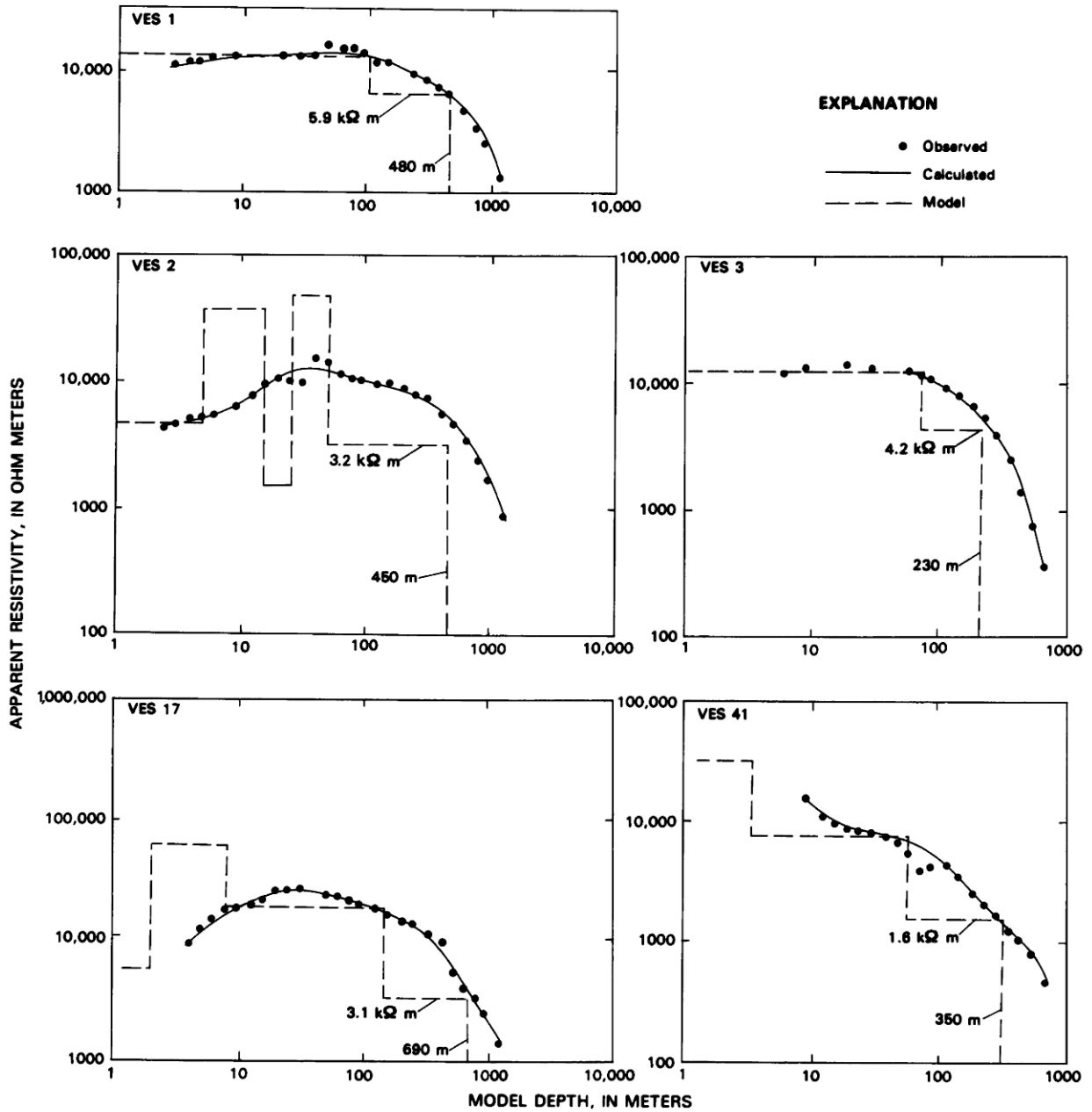


FIGURE 40.8.—Data plots and interpretations for vertical electrical soundings (VES) 1, 2, 3, 17, and 41. See figures 40.1 and 40.11 for locations of soundings. Data for VES 1, 2, and 3 provided by C.J. Zablocki (written commun., 1985).

**UPPER-EAST-RIFT-ZONE PROFILE**

The calculations of apparent water table beneath the UERZ profile (fig. 40.6) shows a generally elevated water table, locally even higher beneath the zone of pit craters. This seems reasonable; the water table is elevated about 610 m above sea level in a research well (location shown in fig. 40.1) about 3.5 km north of the profile

(Zablocki and others, 1974). These water-table elevations are far too high to represent the basal water-table conditions that one expects to find in Hawaii within permeable volcanic rocks where no lateral barriers such as dikes or fault gouge exist (Stearns, 1966). Therefore, the elevated water table must be impounded by high-angle, water-impermeable structures such as dikes. The presence of high-level water outside of the visible surface expression of the rift

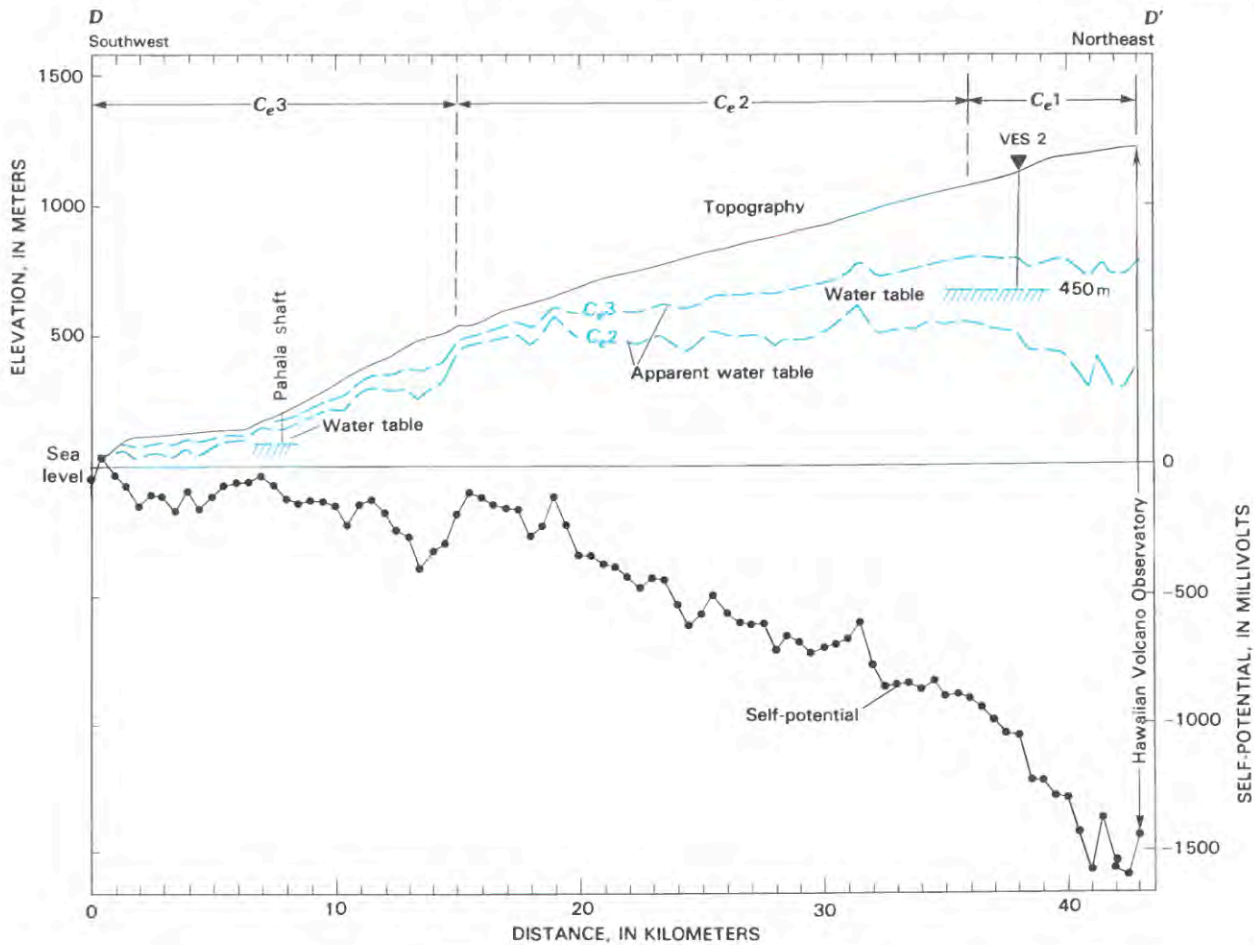


FIGURE 40.9.—Topography, apparent water-table elevations, and self-potential for profile D-D' from Punaluu to the summit (HVO) of Kilauea. An interpretation for VES 2 and the water table in the Pahala shaft are shown for comparison. Segments of the profile that correspond to different linear correlations ( $C_e1$  through  $C_e3$  in fig. 40.10) are indicated. See figure 40.1 for profile location.

zone indicates either that the rift is broader than its surface expression or that faults exist that may be impeding the lateral flow of water.

VES 1 (fig. 40.8, see fig. 40.11 for location) is just within the aeromagnetic anomaly that delineates the northeast boundary of the dike complex (Flanigan and Long, chapter 39). The fact that no short-wavelength SP anomalies (fig. 40.6) occur northeast of the rift suggests that only the southwest side of the rift (coincident with the UERZ line of pit craters) is still active. The elevated water table on the northeast side of the rift can be satisfactorily explained as caused by impoundment by dikes that are now buried and without surface expression. The position at which the elevated water table becomes basal should be the boundary on the northeast side of the rift-zone anomaly. It follows that the northeast boundary of the rift zone is beyond the SP data that we see in figures 40.6 and 40.11. If so, the wavelength of the SP anomaly should be much broader than indicated in either figure 40.6 or 40.11.

VES 17, southwest of the rift, lies outside of the aeromagnetic expression of the dike complex (Flanigan and Long, chapter 39). However, numerous large normal faults of the Koa'e fault system (figs. 40.1 and 40.11) probably act as the hydrologic barrier that elevates the water table beneath VES 17. Either gouge on the Koa'e faults or dikes intruded into the fault planes (in May 1969 for example; see Swanson and others, 1979) from either the SWRZ or the UERZ probably form the actual impermeable part of the hydrologic barrier.

#### SOUTHWEST-RIFT-ZONE PROFILE

The plots of apparent water table (fig. 40.9) indicate that an elevated (nonbasal) water table, which dips to the southwest, underlies the profile between the 28-km and 43-km positions. This inference is supported by ground-water studies near the town of Pahala. Ground water beneath the town stands at approximately 72

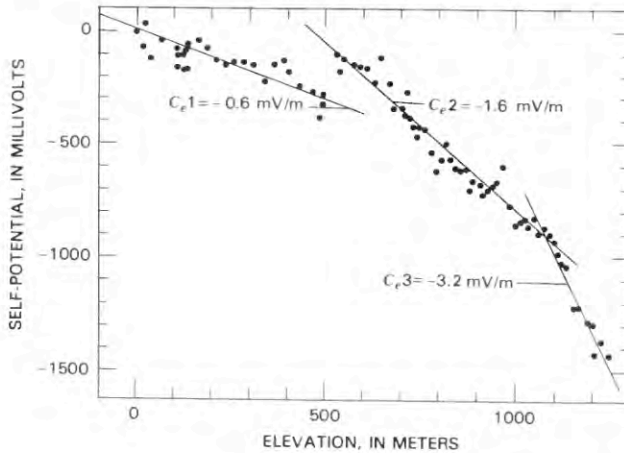


FIGURE 40.10.—Plot of elevation versus self-potential for the 43-km profile shown in figure 40.9. Three gradients,  $C_{e1}$ ,  $C_{e2}$ , and  $C_{e3}$ , show the linear correlations between self-potential and elevation for 3 segments of the profile. Correlation lines are graphically determined.

m above sea level (fig. 40.9) in a Maui-type well (Stearns and Macdonald, 1946) and is probably impounded by older dikes of the SWRZ. Evidence from an electrical sounding survey (Hussong and Cox, 1967) in the immediate area around Pahala indicates that the anomalously high water-table elevation extends to at least 1 km northeast of Pahala (the edge of the study area) and along the highway towards Punaluu. This explains the shallow  $C_e$  gradient ( $C_{e1}$ ) for this part of the profile in figure 40.10.

The portion of the profile between 7-km and 28-km positions appears underlain by a nearly horizontal water table that is at an even higher level than that under the seaward part of the profile. A low-resistivity zone beneath VES 2 (figs. 40.8–40.9) at the 5-km position is interpreted to be the top of the water table; it lies at 450-m depth or about midway between the two plotted apparent water tables. The estimation of water table from SP is only approximate, but the qualitative agreement between the apparent water table and data from the Pahala shaft and VES 2 seems meaningful. Additional determinations of actual water-table elevation would allow a more accurate value of the correlation coefficient of SP and vadose-zone thickness ( $C_e$ ) to be chosen.

### CONCLUSIONS

The edifice of Kilauea sits in a broad self-potential low that appears to be related to negative potentials generated by the percolation of ground water through the vadose zone to the underlying water table. Plots of SP against elevation often have more than one linear segment, which indicates that SP is correlated to something other than elevation. Examination of SP plotted against elevation for profiles where water-table elevation is known indicate the SP correlation is really with vadose-zone thickness rather than with elevation. An empirical gradient of about  $-1.7$  mV per meter

of elevation above sea level seems to best fit the vadose-zone-related potentials along the MERZ and LERZ profiles. A value of  $-3.6$  mV/m appears better for the UERZ profile. A gradient of either  $-1.6$  or  $-3.2$  mV/m may best fit the SWRZ profile; a choice cannot be made without additional data. The observation that the correlation between vadose-zone thickness and SP is not always constant, even when the water table is at a constant elevation, implies the possible addition of potentials related to deep or broad heat sources or possible variation of the parameters of the presumably electrokinetic generating mechanism.

The self-potential profiles, referenced to sea level, have been used to calculate an apparent water-table configuration. Electrical soundings have confirmed the water-table depth directly at critical places and shown places where potentials unrelated to the thickness of the vadose zone must be taken into account.

At only a few locations on the volcano, related to obvious thermal features, do self-potentials become more positive than potential at sea level. On the basis of that observation we are in partial agreement with Zablocki (1978), who conjectured that all

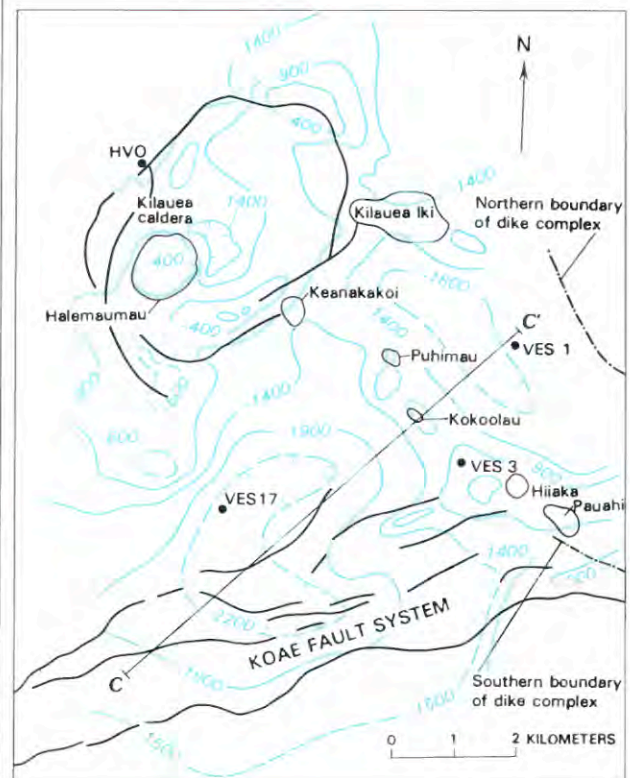


FIGURE 40.11.—Self-potential map of the summit region of Kilauea Volcano (after Zablocki, 1976). Selected contours (blue) show values in millivolts. The potentials are referenced to sea level via the SWRZ profile in figure 40.9. Also shown are the location of profile C-C' and VES 1, 3, and 17 and main geologic features. The northern and southern boundaries of the dike complex defining the east rift zone derived from aeromagnetic studies (Flanigan and Long, chapter 39).

anomalies on Kilauea reflect the distance that water in the vadose zone descends before encountering higher temperature fluids rising above a deeper heat source. Over the rising fluids the more positive potentials (which might still be negative in relation to sea level) reflect (1) a thinner vadose zone and (2) electrokinetic potentials contributed by the rising fluids. We infer, however, that the primary means by which the vadose zone is thinned is high-level impoundment of ground water by dikes in areas known to be loci of intrusions and eruptions on the volcano. The impoundment results in broad anomalies (>3 km) associated with Kilauea's summit and rift zones. The long-wavelength anomalies are not restricted to currently active thermal features but also appear to reflect older dike systems left behind as the rift systems shifted in position to the south. Shorter wavelength anomalies, superimposed on the longer wavelength anomalies, are probably caused by a combination of thermoelectric and electrokinetic effects associated either with specific, recently active fissure vents or with known areas of recent intrusions.

Use of a variety of geophysical techniques combined with observation of recent volcanic activity can contribute to understanding the geologic history of a volcano. An example of this is the UERZ, which is defined by (1) a zone of pit craters on the currently active rift, (2) a broad SP anomaly that extends about 2 km farther to the northeast, and (3) an aeromagnetic anomaly, which is nearly coincident with the SP anomaly. The lack of any high-amplitude narrow-wavelength features in the zone of broad SP and aeromagnetic anomalies northeast of the active rift is consistent with the lack of volcanic activity in that area. The fact that the water table is elevated in this zone indicates that water is impounded northeast of the line of UERZ pit craters by older dikes of the rift system. A second example can be found in the MERZ profile: a rising apparent water table north of the MERZ can best be explained as dike impoundment of ground water by an older dike system of the ERZ or by a postulated inactive branch of the northeast rift zone of Mauna Loa Volcano.

#### REFERENCES CITED

- Anderson, L.A., and Johnson, G.R., 1976, Application of the self-potential method to geothermal exploration in Long Valley, California: *Journal of Geophysical Research*, v. 81, no. 8, p. 1527-1532.
- Corwin, R.F., and Hoover, D.B., 1979, The self-potential method in geothermal exploration: *Geophysics*, v. 44, no. 2, p. 226-245.
- Fitterman, D.V., 1978, Electrokinetic and magnetic anomalies associated with dilatant regions in a layered earth: *Journal of Geophysical Research*, v. 83, p. 5923-5928.
- 1979, Calculations of self-potential anomalies near vertical contacts: *Geophysics*, v. 44, p. 195-205.
- 1983, Modelling of self-potential anomalies near vertical dikes: *Geophysics*, v. 48, no. 2, p. 171-180.
- 1984, Thermoelectrical self-potential anomalies and their relationship to the solid angle subtended by the source region: *Geophysics*, v. 49, p. 165-170.
- Holcomb, R.T., 1980, Preliminary geologic map of Kilauea Volcano, Hawaii: U.S. Geological Survey Open-File Report 80-796, 2 sheets, scale 1:50,000.
- Hussong, D.M., and Cox, D.C., 1967, Estimation of ground-water configuration near Pahala, Hawaii, using electrical resistivity techniques: Water Resources Research Center, University of Hawaii, Technical Report 17, 35 p.
- Jackson, D.B., and Sako, M., 1982, Self potential surveys related to probable geothermal anomalies, Hualalai Volcano, Hawaii: U.S. Geological Survey Open-File Report 82-127, 10 p.
- Keller, G.V., and Frischknecht, F.C., 1966, *Electrical methods in geophysical prospecting*: New York, Pergamon Press, 517 p.
- Klein, D.P., and Larson, J.C., 1978, Magnetic induction fields (2-30 cpd) on Hawaii Island and their implications regarding electrical conductivity in the oceanic mantle: *Royal Astronomical Society Geophysical Journal*, v. 58, no. 53, p. 61-77.
- Lockwood, J.P., Banks, N.G., English, T.T., Greenland, P., Jackson, D.B., Johnson, D.J., Koyanagi, R.Y., McGee, K.A., Okamura, A.T., and Rhodes, M.J., 1985, The 1984 eruption of Mauna Loa Volcano, Hawaii: *Eos, Transactions of the American Geophysical Union*, v. 66, no. 16, p. 169-171.
- Poldini, E., 1939, Geophysical exploration by spontaneous polarization methods: *Mining magazine*, v. 60, p. 22-27.
- Sill, W.R., 1982, Self-potential effects due to hydrothermal convection-velocity crosscoupling: Earth Sciences Laboratory, University of Utah Research Institute, no. DOE/ID/12079-68, 23 p.
- 1983, Self potential modeling from primary flow: *Geophysics*, v. 48, p. 76-86.
- State of Hawaii Department of Land and Natural Resources, 1970, An inventory of basic water resources data—Island of Hawaii: Report R34, 188 p.
- Stearns, H.T., 1966, *Geology of the State of Hawaii*: Palo Alto, California, Pacific Books, 266 p.
- Stearns H.T., and Macdonald, G.A., 1946, Geology and ground water resources of the Island of Hawaii: Hawaii Division of Hydrography Bulletin 9, 363 p.
- Sawson, D.A., Duffield, W.A., Jackson, D.B., and Peterson, D.W., 1979, Chronological narrative of the 1969-71 Mauna Ulu eruption of Kilauea Volcano, Hawaii: U.S. Geological Survey Professional Paper 1056, 55 p.
- Yungul, Sulhi, 1950, Interpretation of spontaneous polarization anomalies caused by spheroidal ore bodies: *Geophysics*, v. 15, no. 2, p. 237-246.
- Zablocki, C.J., 1976, Mapping thermal anomalies on an active volcano by the self-potential method, Kilauea, Hawaii, in *Proceedings, 2nd United Nations Symposium on the Development and Use of Geothermal Resources*, San Francisco, Calif., May 1975, v. 2, p. 1299-1309.
- 1977, Self-potential studies in East Puna, in *Geoelectric studies on the east rift, Kilauea Volcano, Hawaii Island*: Honolulu, Hawaii Institute of Geophysics, University of Hawaii Technical Report HIG-77-15, p. 175-195.
- 1978, Streaming potentials resulting from the descent of meteoric water—a possible source mechanism for Kilauean self-potential anomalies: *Geothermal Resources Council, Transactions*, v. 2, sec. 2, p. 747-748.
- 1980, Observations from self-potential monitoring studies on Kilauea Volcano, Hawaii (1973-1975): U.S. Geological Survey Open-File Report 80-99, 15 p.
- Zablocki, C.J., Tilling, R.I., Peterson, D.W., Christiansen, R.L., Keller, G.V., and Murray, J.C., 1974, A deep research drill hole at the summit of an active volcano, Kilauea, Hawaii: *Geophysical Research Letters*, v. 1, no. 7, p. 23.
- Zohdy, A.A.R., Anderson, L.A., and Muffler, L.J.P., 1973, Resistivity, self-potential and induced polarization surveys of a vapor dominated geothermal system: *Geophysics* v. 38, no. 6, p. 1130-1144.